

Superconvergence Analysis of Gradient Recovery Method for TM Model of Electromagnetic Scattering in the Cavity

Shanghai Jia^{2,1} and Changhui Yao^{1,*}

¹ School of Mathematics and Statistics, Zhengzhou University, Zhengzhou, Henan 450001, China

² School of Statistic and Mathematics, Central University of Finance and Economics, Beijing 100081, China

Received 5 June 2015; Accepted (in revised version) 11 October 2016

Abstract. In this paper, we consider the transform magnetic (TM) model of electromagnetic scattering in the cavity. By the Polynomial Preserving Recovery technique, we present superconvergence analysis for the vertex-edge-face type finite element. From the numerical example, we can see that the provided method is efficient and stable.

AMS subject classifications: 65N06, 65N22

Key words: Scattering, cavity, TM model, gradient recovery method, superconvergence.

1 Introduction

Electromagnetic scattering problems have been considered by many researchers and engineers because of the significant industrial and military applications, which include the design of cavity-backed conformal antennas, the characterization of radar cross-section (RCS) of vehicles with grooves and others [2, 3, 11, 13].

Finite element method is one of the important ways to simulate electromagnetic scattering problems numerically [6, 10, 12, 15, 21, 22, 27]. Some extreme vital focuses should be paid more attentions including that: (1) One has to reduce the infinite problem domain to a bounded computational domain. Many methods have been designed for this purpose including absorbing boundary conditions (ABC) by X. Feng [23], perfectly matched layer (PML) Z. Chen [9, 25, 27], and transparent boundary conditions by G. Bao [13], A. W. Wood [2], K. Du [11] and many references therein. (2) Large wave number problem

*Corresponding author.

Email: shjia@lsec.cc.ac.cn (S. H. Jia), chiyao@lsec.cc.ac.cn (C. H. Yao)

will occur, that is to say, the pollution error of the finite element solution has to be considered in the error analysis. The discontinuous Galerkin (DG) method or CIP-FEM by X. Feng and H. Wu [7,21,22] can deal with such a problem, and hybridizable discontinuous Galerkin (HDG) method provided by H. Chen, P. Lu and X. Xu [15,24] is successful, too.

Theoretically, scattering field in weak formulation belongs to the Sobolev space $H^1(\Omega)$ and its numerical approximation is very worse, even $\mathcal{O}(\epsilon)$, for any $\epsilon > 0$ [5]. Practically, the above numerical ideas were realized, which based on an assumption that scattering fields were filled by materials with proper smooth relative permittivity parameters, seeing D. Arnold [4] and I. Babuska [8]. Therefore, one of facts is that the high convergent order can deduce the effect of large wave number.

Superconvergence analysis is one of excellent post-processing techniques with lower computational costs. The most widely used in practice is Zienkiewicz-Zhus Superconvergence Patch Recovery (SPR) method [16]. However, in [26] the authors showed that the SPR was not superconvergent for linear element under the uniform triangulation with the Chevron pattern grid. The Polynomial Preserving Recovery (PPR) which overcome this restriction was one of the least-squares-based procedures [1].

In this paper, we use PPR with the least-squares-based procedure to improve the convergence order for transverse magnetic (TM) model of Electromagnetic Scattering problem. This method is based on computing a local k order polynomial on a suitable patch associated with each mesh vertex via a discrete least-squares procedure. Then, the nodal gradient can be computed. Numerical example illustrates the effectiveness of this recovery method.

The paper is organized as follows. In Section 2, the TM model in a cavity is provided and the existence and uniqueness of variational problem are presented, too. In Section 3, we formulate vertex-edge-face type finite element and the gradient recovery procedure. In Section 4, superconvergence theory is established. In Section 5, numerical example tests our theories. In Section 6, conclusions in this paper is provided.

2 TM model in a cavity

TM model in a cavity can be formulated by [2,13,20]

$$\begin{cases} \Delta u + k_0^2 \epsilon_r u = f & \text{in } \Omega, \\ u = 0 & \text{on } S, \\ \frac{\partial u}{\partial \mathbf{n}} = T(u) + g & \text{on } \Gamma, \end{cases} \quad (2.1)$$

where $g(x) = -2i\beta e^{i\alpha x}$, and

$$T(u) = \frac{ik_0}{2} \int_0^a \frac{1}{|x-x'|} H_1^{(1)}(k_0|x-x'|) u(x') dx' \quad (2.2)$$

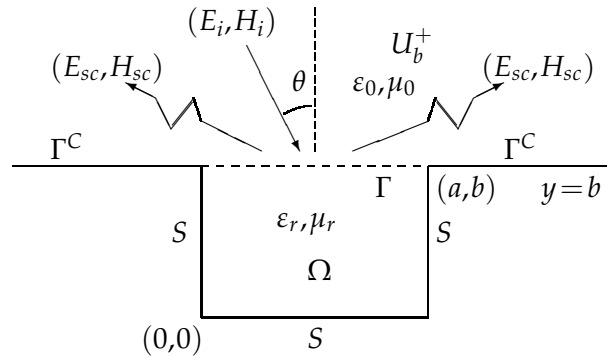


Figure 1: Cavity.

is a Hadamard integral, $H_1^{(1)}$ is the Hankel function. Here we assume that a plane wave $u^i = e^{i\alpha x - i\beta(y-b)}$ is incident on the cavity, where $\alpha = k_0 \sin\theta$, $\beta = k_0 \cos\theta$, $\theta \in (-\pi/2, \pi/2)$. In this model, we also assume that the cavity has a rectangular cross section $\Omega = (0, a) \times (0, b)$. Denote the aperture and the walls of the cavity by $\Gamma = [0, a] \times \{b\}$ and $S = \partial\Omega \setminus \Gamma$, respectively. Let $\mathbb{R}_b = (-\infty, -\infty) \times \{b\}$, $\Gamma^C = \mathbb{R}_b \setminus \Gamma$ and $U_b^+ = \{(x, y) \in \mathbb{R}^2 : y > b\}$, or cf. Fig. 1.

This model is obtained to describe the propagation of the scattered waves from the cavity. By TM polarization, the magnetic field is transferred to the z -axis so that the electric field \mathbf{E} and the magnetic field \mathbf{H} are of the form $\mathbf{E} = (0, 0, E_z)$, $\mathbf{H} = (H_x, H_y, 0)$. To simplify the notation, let $u = E_z(x, y)$ in TM model.

Define the function space

$$H_{00}^{1/2}(\Gamma) = \{u \in H^{1/2}(\Gamma) : \exists \tilde{u} \in H^{1/2}(\mathbb{R}_b), \tilde{u} = 0 \text{ on } \Gamma^C, u = \tilde{u}|_{\Gamma}\}$$

equipped the norm with

$$\|u\|_{H_{00}^{1/2}(\Gamma)} = \|\tilde{u}\|_{H^{1/2}(\mathbb{R})}.$$

Lemma 2.1 (see [14]). *The operator $T : H_{00}^{1/2}(\Gamma) \rightarrow H_{00}^{-1/2}(\Gamma)$ is continuous and for any $u \in H_{00}^{1/2}(\Gamma)$, we have $\text{Re}\langle T(u), u \rangle \leq 0$, $\text{Im}\langle T(u), u \rangle \geq 0$.*

The weak formulation of Eq. (2.1) is: Find $u \in V = \{v \in H^1(\Omega) : v = 0 \text{ on } S, v|_{\Gamma} \in H_{00}^{1/2}(\Gamma)\}$ such that

$$a(u, v) = G(v), \quad \forall v \in V, \tag{2.3}$$

where

$$a(u, v) = \int_{\Omega} (\nabla u \cdot \nabla \bar{v} - k_0^2 \epsilon_r u \bar{v}) dx dy - \int_{\Gamma} T(u) \bar{v} dx, \quad G(v) = \int_{\Gamma} g \bar{v} dx - \int_{\Omega} f \bar{v} dx dy.$$

Lemma 2.2 (see [20]). *Let $u, v \in V$, then there exists positive constant C_i , $i = 0, 1, 2$, such that*

$$|a(u, v)| \leq C_0 \|u\|_1 \|v\|_1, \quad \text{Re}a(u, u) \geq C_1 \|\nabla u\|_0^2 - C_2 \|u\|_0^2. \tag{2.4}$$

Therefore, the variational problem (2.3) has a unique solution $u \in V$.

3 Finite element method and gradient recovery technique

Let \mathcal{T}_h be a quasi-uniform partition of the domain Ω . Define the reference element $\hat{e} = [-1,1] \times [-1,1]$, then there exists an affine mapping F_e from the reference element \hat{e} to a general element e such that

$$\begin{cases} x = x_e + h_x \xi, \\ y = y_e + h_y \eta. \end{cases}$$

Now we can present the *vertex – edge – face* type finite element, whose interpolation of degree k can be given by

$$\begin{cases} \hat{u}_I(\hat{Z}_i) = \hat{u}(\hat{Z}_i), & i = 1, 2, 3, 4, \\ \int_{\hat{l}_i} \hat{u}_I \hat{v} d\hat{s} = \int_{\hat{l}_i} \hat{u} \hat{v} d\hat{s}, & \forall \hat{v} \in \hat{\mathcal{P}}_{k-2}(\hat{l}_i), \quad i = 1, 2, 3, 4, \\ \int_{\hat{e}} \hat{u}_I \hat{v} d\hat{\zeta} d\hat{\eta} = \int_{\hat{e}} \hat{u} \hat{v} d\hat{\zeta} d\hat{\eta}, & \forall \hat{v} \in \hat{\mathcal{Q}}_{k-2}(\hat{e}). \end{cases} \tag{3.1}$$

Here we consider the finite element space

$$V_h = \{v; v|_e = \hat{v} \cdot F^{-1}, \hat{v} \in \hat{\mathcal{Q}}_k(\hat{e}), \forall e \in \mathcal{T}_h\},$$

and we also denote v_I the finite element interpolation of function v by scaling argument from \hat{v}_I .

Therefore, the discrete form of Eq. (2.3) can be formulated: Find $u_h \in V_h^D$ such that

$$a(u_h, v) = G(v), \quad \forall v \in V_h^D, \tag{3.2}$$

where V_h^D denotes the set of the functions in V_h satisfying the boundary condition (2.1).

In the superconvergence theory, it has been proved that this type of interpolation has better superconvergent property than the common Lagrange interpolation especially for high order finite element method. For example, this type of interpolation has very beautiful interpolation expansions by the integral identity or integral expansion [17, 18]. From the definition, we can know there are three kinds of degree of freedom: vertex value, edge integration and face integration. The gradient recovery procedure in this paper aims to obtain these three kinds of degree of freedom.

The gradient recovery procedure can be formulated by the following. Given a finite element solution u_h , we need to define $G_h u_h$ at the following three types of degree of freedom: vertex value, edge integration, and face integration. For the linear element all degrees of freedom are vertex values, for the quadratic element they are vertex values and edge integrations, and for the cubic element all three types of degrees of freedom are presented. After determining values of $G_h u_h$ at all degrees of freedom, we obtain $G_h u_h \in V_h \times V_h$ on the whole domain by interpolation with the original shape functions of V_h .

(1) We start from vertices. For a vertex Z_i , let h_i be the length of the longest edge attached to Z_i . Elements which include Z_i are selected to form the patch ω_i

$$\omega_i = \bigcup_{Z_i \in e \in \mathcal{T}_h} e.$$

Let \mathcal{E}_{Z_i} denote the element edges set on the patch ω_i . We fit a two dimensional polynomial vector of degree k , in the least-squares sense, to the gradient of the finite element solution u_h at the degrees of freedom: edge and face integrations.

In order to eliminate unstability, we implement the recovery process in the reference patch $\hat{\omega}_i$

$$\hat{\omega}_i = F\omega_i = \bigcup_{Z_i \in e \in \mathcal{T}_h} Fe.$$

Then, we set $\widehat{\nabla}u_h(\xi, \eta) = \nabla u_h(x, y)$, $\hat{v}(\xi, \eta) = v(x, y)$. Now, let us define a functional for any polynomial vector $\hat{v} \in (P_k(\hat{\omega}_i))^2$ by

$$\begin{aligned} \mathcal{F}(\hat{v}) = & \sum_{\hat{e} \in \hat{\omega}_i} \sum_{0 < m+j < k-2} \left(\left[\int_{\hat{e}} \hat{v} \cdot (\xi^m \eta^j, 0)^T d\xi d\eta \right]^2 + \left[\int_{\hat{e}} \hat{v} \cdot (0, \xi^m \eta^j)^T d\xi d\eta \right]^2 \right) \\ & + \sum_{\hat{l} \in \hat{\mathcal{E}}_{Z_i}} \sum_{j=0}^{k-1} \left[\int_{\hat{l}} \hat{v} \cdot \hat{\mathbf{t}}_l \hat{s}^j d\hat{s} \right]^2, \end{aligned} \tag{3.3}$$

where $\hat{\mathbf{t}}_l$ denotes the reference unity tangent vector of the corresponding edge and $\hat{\mathcal{E}}_{Z_i}$ denotes the element edges set on the reference patch $\hat{\omega}_i$, and \hat{e} the element in $\hat{\omega}_i$.

In order to implement the recovery procedure, we introduce the following notations

$$\hat{\mathbf{P}}_k = \begin{pmatrix} \hat{\mathbf{P}}_k^T & \mathbf{0}_n^T \\ \mathbf{0}_n^T & \hat{\mathbf{P}}_k^T \end{pmatrix},$$

where

$$\hat{\mathbf{P}}_k^T = (1, \xi, \eta, \xi^2, \dots, \xi^k, \xi^{k-1}\eta, \dots, \eta^k),$$

$\mathbf{0}_n$ denotes the vector whose elements are all zero and $n = (k+1)(k+2)/2 = 3$. The fitting polynomial vector is denoted by

$$\hat{\sigma}_k(\xi, \eta; Z_i) = \hat{\mathbf{P}}_k \hat{\mathbf{a}}$$

with

$$\hat{\mathbf{a}}^T = (\hat{a}_1, \hat{a}_2, \dots, \hat{a}_{2n}).$$

Then, the fitting polynomial vector $\hat{\sigma}_k$ can be determined by minimizing the following functional problem

$$\mathcal{F}(\hat{\sigma}_k - \widehat{\nabla}u_h) = \min_{\hat{v} \in (P_k(\hat{\omega}_i))^2} \mathcal{F}(\hat{v} - \widehat{\nabla}u_h). \tag{3.4}$$

Remark 3.1. In order to reduce the dimensions of the minimization problem (3.4), we can also modify this functional problem into the following similar version

$$\mathcal{F}(\nabla \widehat{\sigma}_{k+1} - \widehat{\nabla} u_h) = \min_{\widehat{v} \in (\mathcal{P}_k(\widehat{\omega}_i))^2} \mathcal{F}(\widehat{v} - \widehat{\nabla} u_h), \tag{3.5}$$

where $\widehat{\sigma}_{k+1} \in P_{k+1}(\widehat{\omega}_i)$.

The minimization problem (3.5) yields the following linear system

$$\widehat{\mathbf{a}} = (A^T A)^{-1} A^T \mathbf{b}_h, \tag{3.6}$$

where

$$A = \begin{bmatrix} 1 & \zeta_1 & \eta_1 & \zeta_1^2 & \cdots & \zeta_1^k & \zeta_1^{k-1} \eta_1 & \cdots & \eta_1^k \\ 1 & \zeta_2 & \eta_2 & \zeta_2^2 & \cdots & \zeta_2^k & \zeta_2^{k-1} \eta_2 & \cdots & \eta_2^k \\ & & & & \cdots & & & & \\ \vdots & \vdots & \vdots & \vdots & \cdots & \vdots & \vdots & \cdots & \vdots \\ 1 & \zeta_n & \eta_n & \zeta_n^2 & \cdots & \zeta_n^k & \zeta_n^{k-1} \eta_n & \cdots & \eta_n^k \end{bmatrix},$$

and the construction of the matrix A can be found in [26] since A has a different form with respect to the degree of finite element spaces. After solving the linear system, we obtain the coefficient vector $\widehat{\mathbf{a}}$ and then the polynomial vector $\widehat{\sigma}_k(\zeta, \eta; Z_i)$. The final fitted polynomial can be obtained by

$$\sigma_k(x, y; Z_i) = \widehat{\sigma}_k\left(\frac{x-x_i}{h}, \frac{y-y_i}{h}; Z_i\right).$$

The condition for (3.6) to have a unique solution is

$$\text{Rank}(A) = 2n, \tag{3.7}$$

which is always satisfied in practical situation when grid points are reasonably distributed. Then, we define

$$G_h u_h(Z_i) = \sigma_k(x, y; Z_i)(Z_i). \tag{3.8}$$

(2) For the degree of freedom on the edge l between two vertices Z_{i_1} and Z_{i_2} , we define

$$\int_l G_h u_h \mathbf{v} ds = \frac{1}{2} \left(\int_l \sigma_k(x_1, y_1, ; Z_{i_1}) \mathbf{v} ds + \int_l \sigma_k(x_2, y_2, ; Z_{i_2}) \mathbf{v} ds \right), \quad \forall \mathbf{v} \in (P_{k-2}(l))^2, \tag{3.9}$$

where (x_1, y_1) (or (x_2, y_2)) is the local coordinate on the edge with origin at Z_{i_1} (or Z_{i_2}).

(3) For the degree of freedom on the element e which formed by four vertices Z_{i_1} , Z_{i_2} , Z_{i_3} and Z_{i_4} . We define

$$\int_e G_h u_h \mathbf{v} dx dy = \frac{1}{4} \sum_{j=1}^4 \int_e \sigma_k(x_j, y_j, ; Z_{i_j}) \mathbf{v} dx dy, \quad \forall \mathbf{v} \in (Q_{k-2}(e))^2, \tag{3.10}$$

where (x_j, y_j) are the local coordinates on the face e with origin at Z_{i_j} , respectively.

4 Superconvergence analysis

In this section, we give the superconvergence analysis of our recovery operator with the tools provided in [17, 18]. First, we find the recovery operator has the following properties.

Theorem 4.1. *The recovery operator G_h defined in this paper satisfies*

$$\|G_h u_h\|_0 \leq C \|u_h\|_1, \quad \forall u_h \in V_h, \quad (4.1a)$$

$$G_h v = \nabla v, \quad \forall v \in \mathcal{P}_{k+1}(\omega_i), \quad (4.1b)$$

$$G_h v = G_h v_I, \quad (4.1c)$$

where v_I is the finite element interpolation of function v scaled by (3.1).

Proof. First, we prove $\mathcal{F}(\hat{v})^{1/2}$ for all $\hat{v} \in (\mathcal{P}_1(\hat{\omega}_i))^2$ on the reference patch $\hat{\omega}_i$. By the property (3.7), we have $\mathcal{F}(\hat{v})^{1/2} = 0$ if and only if $\hat{v} = 0$. And from the finity of the dimension of the polynomial vector space, norm equivalence theorem and the regularity of the partition \mathcal{T}_h , we know there exists constants C_1, C_2 satisfying

$$C_1 \|\hat{v}\|_{0, \hat{\omega}_i} \leq \mathcal{F}(\hat{v})^{1/2} \leq C_2 \|\hat{v}\|_{0, \hat{\omega}_i}.$$

Based on this result and the minimization problem (3.4) or (3.5), we can know

$$\|\hat{\sigma}_k\|_{0, \hat{\omega}_i} \leq 1/C_1 \mathcal{F}(\hat{\sigma}_k)^{1/2} \leq 1/C_1 \mathcal{F}(\widehat{\nabla u_h})^{1/2} \leq C_2/C_1 \|\widehat{\nabla u_h}\|_{0, \hat{\omega}_i}.$$

Together with the definition of the transformation F , the following inequality can be obtained

$$\|\sigma_k\|_{0, \omega_i} \leq C_2/C_1 \|\nabla u_h\|_{0, \omega_i}. \quad (4.2)$$

For any element e , let Z_1, Z_2, Z_3 and Z_4 denote its four vertices. From the recovery process and (4.2) we can obtain the following inequality

$$\|G_h u_h\|_{0, e} \leq C \sum_{i=1}^4 \|\sigma_k(x, y; Z_i)\|_{0, \omega_i} \leq C \sum_{i=1}^4 \|\nabla u_h\|_{0, \omega_i}. \quad (4.3)$$

Then from (4.3) and summing over the mesh, we have

$$\|G_h u_h\|_0^2 = \sum_{e \in \mathcal{T}_h} \|G_h u_h\|_{0, e}^2 \leq C \sum_{e \in \mathcal{T}_h} \sum_{i=1}^4 \|\nabla u_h\|_{0, \omega_i}^2 \leq C \|\nabla u_h\|_0^2.$$

So (4.1a) can be obtained.

For the property (4.1b), we should notice that $\nabla v \in (\mathcal{P}_k(\omega_i))^2$ when $v \in \mathcal{P}_{k+1}(\omega_i)$ on a patch ω_i . From the function definition (3.3) and the minimizing function problem (3.4),

we know the fitting polynomial $\sigma_k(x,y;;Z_i) = \nabla v$ on a patch ω_i , then the property (4.1b) can be obtained.

For (4.1c), we need to prove $G_h(v - v_I) = 0$. This can be ensured by

$$\int_l \frac{\partial(v - v_I)}{\partial \mathbf{t}_l} \varphi ds = (v - v_I) \varphi \Big|_{Z_{i_1}}^{Z_{i_2}} - \int_l (v - v_I) \frac{\partial \varphi}{\partial \mathbf{t}_l} ds = 0, \quad \forall \varphi \in P_{k-1}(l),$$

and

$$\int_e \nabla(v - v_I) \cdot \mathbf{w} dx dy = \int_{\partial e} (v - v_I) \cdot \mathbf{n} w ds - \int_e (v - v_I) \cdot \nabla \cdot \mathbf{w} dx dy = 0, \quad \forall \mathbf{w} \in P_{k-2}(e),$$

for each edge l between Z_{i_1} and Z_{i_2} and each element e . □

This is a smart representation for the definition of the vertex-edge-face interpolation and shows that the recovery method has the property (4.1c).

Based on Theorem 4.1, we can obtain the superconvergence result after recovering the gradient.

Theorem 4.2. *Assume that the partition is uniform and the regularization of the solution is $H^{k+1+\delta}(\Omega) \cap H^{k+2}(\Omega)$. If the following superclose exists*

$$\|u_h - u_I\|_1 \leq Ch^{k+1+\delta}, \tag{4.4}$$

where $\delta \in (0,1]$. Then, we have the superconvergence result

$$\|G_h u_h - \nabla u\|_0 \leq Ch^{k+1+\delta}. \tag{4.5}$$

Proof. Since $G_h u \in \mathcal{P}_{k+1}$, we have $\|G_h u - \nabla u\|_0 \leq ch^{k+2}$. Combining Theorem 4.1 and (4.4), we have

$$\begin{aligned} \|G_h u_h - \nabla u\| &\leq \|G_h u_h - G_h u_I\|_0 + \|G_h u_I - G_h u\|_0 + \|G_h u - \nabla u\|_0 \\ &\leq C \|u_h - u_I\|_1 + Ch^{k+2} \\ &\leq Ch^{k+1+\delta}. \end{aligned}$$

This is the desired result and we complete the proof. □

5 Numerical example

Consider a cavity $\Omega = (0,1) \times (0,1)$, and select $f_M(x,y)$ and $g_M(x)$ such that (2.1), has the exact solution

$$u(x,y) = e^{xy} \sin(k_0 x) \sin\left(\left(k_0 + \frac{\pi}{2}\right)y\right).$$

Table 1: The results for $k_0=4\pi, 8\pi$ by using Q_1 .

N	$k_0=4\pi$				$k_0=8\pi$			
	err_h	$rate_h$	err_{G_h}	$rate_{G_h}$	err_h	$rate_h$	err_{G_h}	$rate_{G_h}$
16	3.1510	-	4.9515	-	11.9593	-	22.5058	-
32	1.5649	1.0097	1.4073	1.8150	5.9065	1.0178	9.1237	1.3026
64	0.7807	1.0032	0.3632	1.9542	2.9277	1.0125	2.5872	1.8182
128	0.3901	1.0009	0.0914	1.9902	1.4598	1.0040	0.6676	1.9544
256	0.1950	1.0002	0.0229	1.9986	0.7293	1.0011	0.1681	1.9894

Table 2: The results for $k_0=16\pi, 32\pi$ by using Q_1 element.

N	$k_0=16\pi$				$k_0=32\pi$			
	err_h	$rate_h$	err_{G_h}	$rate_{G_h}$	err_h	$rate_h$	err_{G_h}	$rate_{G_h}$
64	11.4507	-	17.4649	-	45.8078	-	84.7172	-
128	5.6693	1.0142	4.9608	1.8158	22.5576	1.0220	34.1448	1.3110
256	2.8258	1.0045	1.2810	1.9533	11.1611	1.0151	9.7147	1.8134
512	1.4117	1.0012	0.3228	1.9886	5.5619	1.0048	1.0048	1.9525

Define

$$err_h = \|\nabla u - \nabla u_h\|_{0,\Omega}, \quad rate_h = \frac{\log(err_h / err_{h/2})}{\log 2},$$

$$err_{G_h} = \|G_h u_h - \nabla u\|_{0,\Omega}, \quad rate_{G_h} = \frac{\log(err_{G_h} / err_{G_h/2})}{\log 2}.$$

By using bilinear finite element Q_1 , we have the following results in Table 1 and Table 2, where N is the partition number of the cavity. We employ the Q_2 element so that the pollution effect are deduced by PPR efficiently, which can be seen from the error results of err_{G_h} in Tables 3-6 and Figs. 2-3.

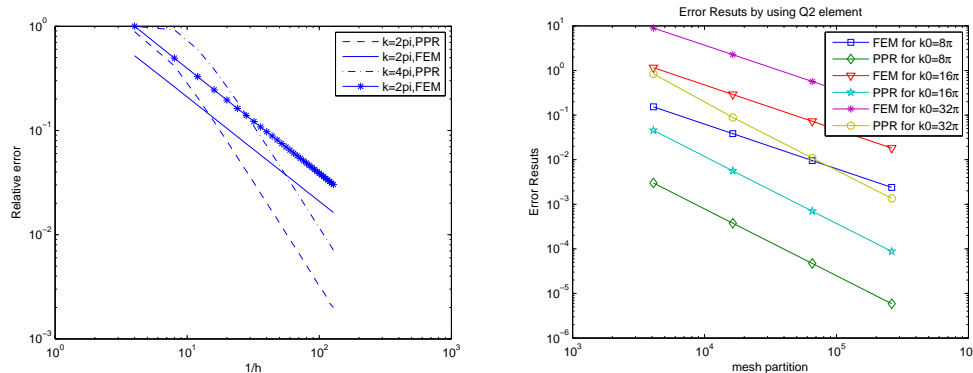


Figure 2: Left: The relative error of $G_h u_h$ and ∇u_h for $k=2\pi, 4\pi$ by using Q_1 element. Right: The error results for FEM and PPR by using Q_2 element.

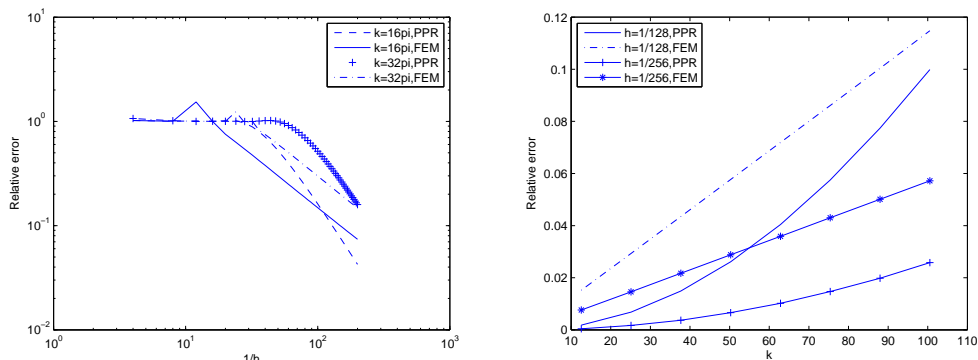


Figure 3: Left: The relative error of $G_h u_h$ and ∇u_h for $k=2\pi, 4\pi$. Right: The relative error results for $h=1/256$ and $1/512$ by running PPR and FEM.

6 Conclusions

By analyzing the Polynomial Preserving Recovery technique, we find that the *vertex – edge – face* type finite element can reduce the effect of high wave number and improve the

Table 3: The results for $k_0 = 4\pi$ by using Q_2 element.

N	$k_0 = 4\pi$			
	err_h	$rate_h$	err_{G_h}	$rate_{G_h}$
64	0.021456155491035	-	0.000218448176029	-
128	0.005364772691266	1.999802647978803	0.000027331205045	2.998670084370496
256	0.001341284738417	1.999901508051906	0.000003417649365	2.999472774589832
512	0.000336107218409	1.996622104201583	0.000000427270047	2.999784303175604

Table 4: The results for $k_0 = 8\pi$ by using Q_2 element.

N	$k_0 = 8\pi$			
	err_h	$rate_h$	err_{G_h}	$rate_{G_h}$
64	0.153220340469570	-	0.003006197045738	-
128	0.038325256878684	1.999240465332771	0.000375805078575	2.999883107611960
256	0.009582572384201	1.999810565803481	0.000046994078816	2.999433667348499
512	0.002395762883155	1.999927864070441	0.000005875329047	2.999737433862963

Table 5: The results for $k_0 = 16\pi$ by using Q_2 element.

N	$k_0 = 16\pi$			
	err_h	$rate_h$	err_{G_h}	$rate_{G_h}$
64	1.161091062136408	-	0.045770998116931	-
128	0.290876070724070	1.997004603075570	0.005615671166158	3.026903388669113
256	0.072755743374847	1.999271571548182	0.000701003968984	3.001963941292057
512	0.018191229428450	1.999818090802620	0.000087617790109	3.000126879940013

Table 6: The results for $k_0 = 32\pi$ by using Q_2 element.

N	$k_0 = 32\pi$			
	err_h	$rate_h$	err_{G_h}	$rate_{G_h}$
64	8.980344904299908	-	0.846370335183954	-
128	2.265434789646899	1.986982891415834	0.088603130354520	3.255859487362545
256	0.567506228571475	1.997079831925783	0.010873141162294	3.026588886717359
512	0.141946674795954	1.999287173275054	0.001356424608777	3.002888014720816

convergent accuracy. The superconvergence theory can be extended to the Polynomial Preserving Recovery method, too. The provided method can also be applied to triangular finite element [19]. And quadrilateral finite element can also be explored by the same way.

Acknowledgments

All the authors would like to thank Prof. K. Du (School of Mathematical Sciences, Xiamen University) for his help. The first author would like to thank NSFC (Nos. 11571389 and 11201501) and the Program for Innovation Research in Centre University of Finance and Economics. The second author would like to thank NSFC (Nos. 11471296 and 11101384).

References

- [1] A. NAGA AND Z. ZHANG, *A posteriori error estimates based on the polynomial preserving recovery*, SIAM J. Numer. Anal., 42(4) (2004), pp. 1780–1800.
- [2] A. W. WOOD, *Analysis of electromagnetic scattering from an overfilled cavity in the ground plane*, J. Comput. Phys., 215 (2006), pp. 630–641.
- [3] B. ALAVIKIA AND O. M. RAMAHI, *Finite-element solution of the problem of scattering from cavities in metallic screens using the surface integral equation as a boundary constraint*, J. Opt. Soc. Am. A, 26 (2009), pp. 1915–1925.
- [4] D. ARNOLD, *An interior penalty finite element method with discontinuous elements*, SIAM J. Numer. Anal., 19 (1982), pp. 742–760.
- [5] D. ZHANG, *Study of Some Electromagnetic Scattering and Inverse Scattering Problem for Chiral Media*, Phd. thesis, University of Jilin, 2004.
- [6] G. BAO, *Finite element approximation of time harmonic waves in periodic structures*, SIAM J. Numer. Anal., 32(4) (1995), pp. 1155–1169.
- [7] L. ZHU AND H. WU, *Pre-asymptotic error analysis of CIP-FEM and FEM for Helmholtz equation with high wave number part II: hp version*, SIAM J. Numer. Anal., 51 (2013), pp. 1828–1852.
- [8] I. BABUSKA AND M. SURI, *The hp version of the finite element method with quasiuniform meshes*, Math. Model. Numer. Anal., 21 (1987), pp. 199–238.
- [9] J. LI AND Y. HUANG, *Time-Domain Finite Element Methods for Maxwell's Equations in Metamaterials*, Springer Series in Computational Mathematics, Vol. 43, Springer, 2013.

- [10] J. HUANG, A. W. WOOD AND MICHAEL J. HAVRILLA, *A hybrid finite element-Laplace transform method for the analysis of transient electromagnetic scattering by an over-filled cavity in the ground plane*, Commun. Comput. Phys., 5(1) (2009), pp. 126–141.
- [11] K. DU, *Two transparent boundary conditions for the electromagnetic scattering from two-dimensional overfilled cavities*, J. Comput. Phys., 230 (2011), pp. 5822–5835.
- [12] K. DU, W. SUN AND X. ZHANG, *Arbitrary high-order $C0$ tensor product Galerkin finite element methods for the electromagnetic scattering from a large cavity*, J. Comput. Phys., 242 (2013), pp. 181–195.
- [13] H. AMMARI, G. BAO AND A. W. WOOD, *An integral equation method for the electromagnetic scattering from cavities*, Math. Methods Appl. Sci., 23 (2000), pp. 1057–1072.
- [14] H. AMMARI, G. BAO AND A. W. WOOD, *Analysis of the electromagnetic scattering from a cavity*, Japan J. Ind. Appl. Math., 19 (2002), pp. 301–310.
- [15] H. CHEN, P. LU AND X. XU, *A hybridizable discontinuous Galerkin method for the Helmholtz equation with high wave number*, SIAM J. Numer. Anal., 51(4) (2013), pp. 2166–2188.
- [16] O. C. ZIENKIEWICZ AND J. Z. ZHU, *The superconvergence patch recovery and a posteriori error estimates, part 1: The recovery technique*, Int. J. Numer. Methods Eng., 33 (1992), pp. 1331–1364.
- [17] Q. LIN AND J. LIN, *Finite Element Methods: Accuracy and Improvement*, China Sci. Tech. Press, 2005.
- [18] Q. LIN AND N. YAN, *The Construction and Analysis of High Efficiency Finite Element Methods*, HeBei University Publishers, China, 1995.
- [19] Q. LIN AND H. XIE, *Superconvergence measurement for general meshes by linear finite element method*, Math. Practice Theory, 41(1) (2011), pp. 138–152 (in Chinese).
- [20] TRI VAN AND A. W. WOOD, *Finite element analysis of electromagnetic scattering from a cavity*, IEEE. Trans. Antennas Propagation, 51(1) (2003), pp. 130–137.
- [21] X. FENG AND H. WU, *Discontinuous Galerkin methods for the Helmholtz equation with large wave numbers*, SIAM J. Numer. Anal., 47 (2009), pp. 2872–2896.
- [22] X. FENG AND H. WU, *hp-discontinuous Galerkin methods for the Helmholtz equation with large wave number*, Math. Comput., 80 (2011), pp. 1997–2024.
- [23] X. FENG, *Absorbing boundary conditions for electromagnetic wave propagation*, Math. Comput., 68(225) (1999), pp. 145–168.
- [24] X. FENG AND Y. XING, *Absolutely stable local discontinuous Galerkin methods for the Helmholtz equation with large wave number*, Math. Comput., 82 (2013), pp. 1269–1296.
- [25] Y. HUANG AND J. LI, *Numerical analysis of a PML model for time-dependent Maxwell's equations*, J. Comput. Appl. Math., 235 (2011), pp. 3932–3942.
- [26] Z. ZHANG AND A. NAGA, *A new finite element gradient recovery method: Superconvergence property*, SIAM J. Sci. Comput., 26(4) (2005), pp. 1192–1213.
- [27] Z. CHEN AND H. WU, *An adaptive finite element method with perfectly matched absorbing layers for the wave scattering by periodic structures*, SIAM J. Numer. Anal., 41 (2003), pp. 799–826.